Published in final edited form as:
Int J Biochem Cell Biol. 2012 December ; 44(12): 2204–2211. doi:10.1016/j.biocel.2012.09.004.

A relatively low level of ribosome depurination by mutant forms of ricin toxin A chain can trigger protein synthesis inhibition, cell signaling and apoptosis in mammalian cells

Amanda E. Jetzt[a], **Ju-Shun Cheng**[a], **Xiao-Ping Li**[b], **Nilgun E. Tumer**[b], and **Wendie S. Cohick**[a,*]

[a]Department of Animal Sciences, 59 Dudley Road, Rutgers, The State University of NJ, New Brunswick NJ 08901-8520 USA

[b]Department of Plant Biology and Pathology, School of Environmental and Biological Sciences, 59 Dudley Road, Rutgers, The State University of NJ, New Brunswick NJ 08901-8520 USA

Abstract

The A chain of the plant toxin ricin (RTA) is an *N*-glycosidase that inhibits protein synthesis by removing a specific adenine from the 28S rRNA. RTA also induces ribotoxic stress, which activates stress-induced cell signaling cascades and apoptosis. However, the mechanistic relationship between depurination, protein synthesis inhibition and apoptosis remains an open question. We previously identified two RTA mutants that suggested partial independence of these processes in a yeast model. The goals of this study were to establish an endogenous RTA expression system in mammalian cells and utilize RTA mutants to examine the relationship between depurination, protein synthesis inhibition, cell signaling and apoptosis in mammalian cells. The non-transformed epithelial cell line MAC-T was transiently transfected with plasmid vectors encoding precursor (pre) or mature forms of wild-type (WT) RTA or mutants. PreRTA was glycosylated indicating that the native signal peptide targeted RTA to the ER in mammalian cells. Mature RTA was not glycosylated and thus served as a control to detect changes in catalytic activity. Both pre- and mature WT RTA induced ribosome depurination, protein synthesis inhibition, activation of cell signaling and apoptosis. Analysis of RTA mutants showed for the first time that depurination can be reduced by 40% in mammalian cells with minimal effects on inhibition of protein synthesis, activation of cell signaling and apoptosis. We further show that protein synthesis inhibition by RTA correlates more linearly with apoptosis than ribosome depurination.

Keywords

ricin toxin A chain; mutants; ribosome depurination; apoptosis; signal transduction; mammalian cells

*Corresponding author at Department of Animal Sciences, 59 Dudley Road, Rutgers, the State University of NJ, New Brunswick NJ 08901-8520. Tel: 1-848-932-6319 Fax 1-732-932-6996. cohick@aesop.rutgers.edu.

1. Introduction

The plant toxin ricin is produced by the castor bean plant *Ricinus communis* and belongs to a family of ribosome-inactivating proteins (RIPs). Its severe toxicity and wide availability has led to its use as an agent of bioterrorism (Rainey and Young, 2004, Audi et al., 2005). In addition, ricin has been investigated as the active moiety of immunotoxins selectively targeted to cancer cells (Castelletti et al., 2004, Schindler et al., 2011, Zhou et al., 2010). Ricin is composed of two subunits which are encoded by a single gene. The catalytically active A subunit (RTA) depurinates a specific adenine in the α-sarcin/ricin loop (SRL) of the 28S rRNA, resulting in protein synthesis inhibition (Sandvig and van Deurs, 2005, Watson and Spooner, 2006). The B subunit (RTB) binds to cell surface receptors through galactose and *N*-acetyl galactosamine moieties. After internalization, ricin is transported from early endosomes to the endoplasmic reticulum (ER) via the trans-Golgi network (Spooner and Lord, 2012). While active research is underway to develop effective vaccines (Marsden et al., 2004, Smallshaw et al., 2007, Smallshaw and Vitetta, 2012, Vitetta et al., 2006), monoclonal antibodies (Dai et al., 2011) and small molecule inhibitors (Pang et al., 2011, Pruet et al., 2011, Stechmann et al., 2010, Wahome et al., 2010) to prevent or treat ricin toxicity, there are currently no approved antidotesor therapeutics available.

The ability to develop effective antidotes against ricin or to use it as the active component of an immunotoxin hinges on a thorough understanding of its biological actions in mammalian cells. In addition to its inhibitory effect on protein synthesis, ricin also induces apoptosis in multiple cell types *in vitro* and *in vivo* (Tesh, 2012). Ricin triggers the intrinsic apoptotic pathway as evidenced by release of cytochrome c from mitochondria and subsequent activation of caspase 3, caspase 9 and PARP (Hu et al., 2001, Jetzt et al., 2009, Rao et al., 2005). However, the role of ribosome depurination and protein synthesis inhibition in the apoptotic response remains unclear. The finding that protein synthesis inhibitors that act on the 28S rRNA (i.e. anisomycin and ricin) activate caspase 3 while protein synthesis inhibitors with a different mechanism of action (i.e. diphtheria toxin and cycloheximide) do not suggests that the mode of protein synthesis inhibition may influence the induction of apoptosis (Kageyama et al., 2002). In addition to its inhibitory effect on protein synthesis, ricin also activates the signaling cascades JNK and p38 (Iordanov et al., 1997, Jetzt et al., 2009, Korcheva et al., 2007). The ability to activate these pathways requires a ribosome that is translationally active, indicating that the ribosome actively senses damage to the 28S rRNA. This has been termed the ribotoxic stress response (Iordanov et al., 1997). We have shown that inhibiting the JNK pathway attenuates the ability of RTA to induce apoptosis in MAC-T cells (Jetzt et al., 2009), while the p38 pathway has been shown to play a role in the proinflammatory cytokine response that is observed with ricin toxicity (Higuchi et al., 2003, Korcheva et al., 2007, Lindauer et al., 2010). Although activation of the ribotoxic stress response by ricin clearly triggers signaling cascades involved in apoptosis, the precise role of this response as it relates to protein synthesis inhibition has not been established.

We previously conducted chemical mutagenesis of the precursor form of RTA (preRTA) which contains a 35-residue leader peptide and isolated mutants based on their inability to induce cell death. Two mutants were identified (P95L/E145K and S215F) that depurinate ribosomes and inhibit protein synthesis similar to WT RTA at 6 h post induction. However, these mutants failed to induce nuclear fragmentation and reactive oxygen species (ROS) generation, which are apoptotic-like characteristics in yeast (Li et al., 2007). These data provide support for the concept that the level of depurination and protein synthesis inhibition may not correspond with cell death. To investigate these relationships in mammalian cells, WT RTA and RTA mutants that caused different levels of depurination in yeast were expressed in MAC-T cells. RTA mutants included the two mentioned above (i.e. P95L/E145K and S215F), G212E, which has very low enzymatic activity and is not toxic in yeast

and RTA active site mutants E177K and E177Q. Since the preRTA gene containing the leader sequence would target RTA to the ER, the mature RTA gene lacking the leader sequence was also expressed to examine direct effects of the mutations on catalytic activity in the absence of ER trafficking.

2. Materials and Methods

2.1. Reagents

Insulin, gentamicin, D-(+)-glucose, RTA purified from *Ricinus communis* and phenol red-free Dulbecco's modified Eagle's medium (DMEM) with low glucose were purchased from Sigma-Aldrich (St. Louis, MO). DMEM containing 4.5 g/l D-glucose (i.e. DMEM-H) and penicillin/streptomycin were obtained from Invitrogen (Carlsbad, CA). Fetal bovine serum (FBS) was purchased from Atlanta Biologicals (Lawrenceville, GA). Endoglycosidase H was obtained from New England Biolabs (Ipswich, MA). Recombinant RTA with N-terminal histidine tag expressed in *E. coli* (NR-853) was obtained through NIAID NIH Biodefense and Emerging Infections (BEI) Research Resources Repository (Manassas, VA). Anti-RTA antibody was produced in rabbits (Covance Research Products; Denver, PA). Antibodies against JNK, p38 and phospho-p38 were purchased from Cell Signaling Technology (Danvers, MA) and phospho-JNK antibody was obtained from Santa Cruz Biotechnology (Santa Cruz, CA). Donkey anti-rabbit and horse anti-mouse horseradish peroxidase-linked secondary antibodies were purchased from GE Healthcare (Piscataway, NJ) and Vector Laboratories (Burlingame, CA), respectively. Peroxidase activity was detected by Pierce ECL Western Blotting Substrate (Thermo Scientific, Rockford, IL) or ECL Prime (GE Healthcare).

2.2 Mutant RTA plasmid construction

The coding sequence of *Ricinus communis* preRTA containing the 35-residue leader sequence (Piatak et al., 1988) was converted to an optimized codon usage for *Bos taurus* (Fig. S1) and synthesized. Mature RTA lacking the leader sequence was then constructed from preRTA by PCR cloning (Genscript; Piscataway, NJ). Genes were subcloned into pCAGGS mammalian expression vector (Niwa et al., 1991). Site-directed mutagenesis was performed using the QuikChange Lightning Site-Directed Mutagenesis Kit (Stratagene; La Jolla, CA). The locations of individual mutations are shown in Figure 1. Mutagenesis was confirmed by sequencing. Constructs for transfection were prepared using an EndoFree Plasmid Maxi Kit (Qiagen; Valencia, CA).

2.3. Cell culture

The bovine mammary epithelial cell line MAC-T (Huynh et al., 1991) was maintained as previously described (Fleming et al., 2005). For all experiments MAC-T cells were plated in phenol-red free DMEM containing 4.5 g/l D-glucose (DMEM-H), 10% FBS, 20 U/ml penicillin, 20 μg/ml streptomycin, and 50 μg/ml gentamicin (complete media). The human epithelial cell line HEK293T/17 was obtained from ATCC (Manassas, VA). HEK293T/17 cells were maintained and plated for experiments in complete media with phenol red and without gentamicin. All cells were cultured at 37°C in a humidified environment with 5% CO_2.

2.4. Transfection

MAC-T cells were plated in complete media at 3.5×10^4 cells/cm^2. The next day subconfluent cells were transfected with endotoxin-free plasmid DNA and SuperFect (Qiagen) combined in a 1:5 ratio for 60 × 15 mm dishes and in a 1:10 ratio for 96 well plates. The transfection mixture was prepared in DMEM-H with no additives, vortexed for 10 sec, and incubated at RT for 10 min. Spent media was removed from cells and replaced

with fresh complete media and the transfection mixture. After 3 h media was removed and replaced with fresh complete media. HEK293T/17 cells were plated at $5 \times 10^4/cm^2$. The following day, subconfluent cells were transfected with endotoxin-free plasmid DNA and GeneJuice (EMD Chemicals Inc.; San Diego, CA) according to the manufacturer's protocol. Transfection efficiencies for both cell lines were monitored using pEGFP (Clontech, Mountain View, CA).

2.5. Western immunoblotting

MAC-T or HEK293T/17 cells were plated in 60 × 15 mm dishes at 3.5×10^4 cells/cm^2 or 5×10^4 cells/cm^2, respectively, and transfected the next day as described above. After incubation in serum-containing media for the indicated times cells were washed twice with cold PBS and total cell lysates were collected by scraping into cold cell lysis buffer as previously described (Grill et al., 2002). Cells were then incubated on ice at 4°C for 30 min and spun at 1000 × g for 5 min at 4°C. The supernatant was removed and passed ten times through an 18 gauge needle. The cell lysates were aliquoted and stored at −80°C until use. Protein concentration was determined using the Bio-Rad Protein Assay (Bio-Rad; Hercules, CA). To determine glycosylation status of expressed RTA, cell lysates were denatured at 100°C for 10 min and incubated with Endoglycosidase H (25 U/mg) at 37°C for 1 h. Proteins were separated by SDS-PAGE and transferred to 0.45 μm PVDF (Millipore, Billerica, MA) or 0.2 μm nitrocellulose (Bio-Rad).

2.6. rRNA depurination assays

MAC-T cells were plated in 60 × 15 mm dishes at 3.5×10^4 cells/cm^2 and transfected the following day as described above. After transfection cells were scraped into 1 ml Trizol (Invitrogen) and stored at −80°C. Total RNA was purified using RNeasy columns (Qiagen). rRNA depurination was then analyzed by dual primer extension analysis as described previously (Jetzt et al., 2009).

rRNA depurination was also analyzed by quantitative reverse transcription PCR (qRT-PCR) as previously described (Melchior and Tolleson, 2010) with minor modifications. Briefly, total RNA (2 μg) was reverse transcribed into cDNA using the High Capacity cDNA Reverse Transcription (RT) kit (Applied Biosystems, Carlsbad, CA). RT reactions (20 μl total volume) were incubated at 25 C for 10 min, 37°C for 2 h, and 85°C for 5 min, and stored at −20°C. Quantitative PCR was performed in a StepOnePlus Real-Time PCR System (Applied Biosystems). Each RT reaction was diluted 1:500 and assayed in triplicate. Total reaction volume (20 μl) contained 5 μl of cDNA, 0.5 μl of each primer, 10 μl *Power* SYBR Green PCR Master Mix (Applied Biosystems) and 4 μl nuclease-free water. Primers (Sigma) that recognize bovine 28S rRNA and the depurination (dep) fragment were designed as described by Melchior and Tollensen (2010). Primers were 28S-F, 5′-GATGTTGGCTCTTCCTATCATTGT-3′; 28S-R, 5′-CCAGCTCACATGCCCTATTAGTT-3′; dep-F, 5′-TGCCATGGTACCTGCTCAGCA-3′; dep-R, 5′-TCTGAACCTGTGGTTCCACA-3′. Final primer concentrations were 0.25 μM except for dep-R which was 0.75 μM. Cycling conditions were 95°C for 10 min followed by 35 cycles of 95°C for 15 sec and 60°C for 1 min. Melting curves were generated for each sample. Each primer set was validated by constructing standard curves using serial dilutions (1:50 to 1:500,000) of an RT reaction derived from RNA collected from MAC-T cells treated for 6 h with RTA (1 μg/ml). The calculated amplification efficiencies were 95.8% ± 1.3 for the 28S primer pair and 95.4% ± 0.2 for the depurination primer pair (mean ± SD for three independent curves). Treatment effects were determined as fold-change using the $\Delta\Delta C_T$ method. The average C_T value for reactions containing 28S (endogenous reference) primers was subtracted from the average C_T value for reactions containing depurination primers for that same sample (ΔC_T). The same calculation was preformed for a calibrator

sample (vector control). The $\Delta\Delta C_T$ was then determined by subtracting the ΔC_T of a calibrator sample (vector control) from the ΔC_T of each test sample.

2.7. Protein synthesis inhibition assay

MAC-T cells were plated in black 96-well plates at 3.5×10^4 cells/cm^2 and transfected the following day as described above. Cells were co-transfected with equal amounts of RTA mutant and pEGFP-N1 reporter plasmid. Twenty-one hours after the start of transfection the EGFP fluorescent signal was measured in a plate reader (BioTek) with excitation filter 485/20 and emission filter 530/25. Fluorescence measured in cells co-transfected with GFP and empty vector was considered 100%.

2.8. Caspase 3/7 assay

Cells were plated in black 96-well plates at 3.5×10^4 cells/cm^2 and transfected the following day as described above. Caspase 3/7 activation was determined using the SensoLyte Homogeneous AMC Caspase 3/7 Assay Kit from AnaSpec (San Jose, CA) as described by the manufacturer.

2.9. Nucleosome accumulation assay

Cells were plated in 96-well plates at 3.5×10^4 cells /cm^2 and transfected the following day as described above. Nucleosome accumulation was determined using the Cell Death Detection ELISA kit (Roche Applied Science, Indianapolis, IN) as described by the manufacturer.

2.10. Statistical analysis

Data were analyzed by one-way ANOVA with Dunnett's Multiple Comparison Test. PreRTA mutants were compared to WT preRTA while mature RTA mutants were compared to WT mature RTA. Differences were considered significant for $P < 0.05$. Analyses were performed using GraphPad Prism (5.02).

3. Results

3.1. The native signal peptide targets RTA to the ER in mammalian cells

The *Ricinus communis* gene encoding RTA was modified to utilize preferred codons for the bovine in order to optimize expression of pre- and mature RTA in the MAC-T cell line. The preRTA contained the native 35-residue N-terminal leader peptide followed by the 267-residue mature RTA, while mature RTA did not contain the leader peptide (Fig. 1A). A comparison of the two sequences is shown in Fig. S1. Point mutations were then introduced to create RTA mutants that we had previously shown to decrease cytotoxicity in yeast (Li et al., 2007) (Fig. 1A, B). MAC-T cells were transiently transfected with either pre- or mature forms of WT and mutant RTA. As shown in Fig. 2A, the mature WT protein and all seven mature RTA mutants were detectable by western blotting with an RTA antibody although the mature double mutant P95L/E145K was very faint. All preRTA forms were easily detectable with the exception of E145K and P95L/E145K. The latter two mutants were only visible with much longer exposure times. To determine if higher expression of E145K and the double mutant could be obtained by transfecting a different cell line, HEK293T/17 cells were transfected with the codon-optimized RTA-expressing vectors. As shown in Fig. S2, the pattern of expression for pre- and mature WT, E177K, E145K and the double mutant was similar in HEK293T/17 cells to that observed in MAC-T cells. Pre- and mature E177K were more abundantly expressed than the other RTA forms in both MAC-T and HEK293T/17 cells.

RTA is *N*-glycosylated on asparagine residues 10 and 236 (Rutenber et al., 1991) in the ER (Rapak et al., 1997). The first 26 residues of the 35-residue N-terminal leader peptide target RTA to the ER in yeast (Yan et al., 2012) and in plants (Halling et al., 1985). PreRTA ran as a doublet of approximately 30 and 32 kDa which corresponded with the molecular weight of the doublet observed for glycosylated RTA purified from *Ricinus communis.* Mature RTA ran as a single band at approximately 30 kDa similar to non-glycosylated recombinant RTA (Fig. 2B). To determine if the differences in size were due to glycosylation, lysates collected from cells transfected with pre- or mature WT and E177K were treated with Endoglycosidase H (Endo H) which cleaves the *N*-linked mannose groups of oligosaccharides (Fig. 2C). The doublet observed in cells expressing the pre-form of RTA or E177K was reduced to one band after Endo H treatment. The single band observed in cells transfected with mature RTA and E177K did not change in size with Endo H treatment. These data demonstrate that the signal sequence of native RTA from the castor bean plant successfully targets the precursor form of RTA to the ER in MAC-T cells. In contrast, expression of the mature form resulted in nonglycosylated RTA, indicating that it is not translocated into the ER.

3.2. Ribosome depurination and protein synthesis inhibition are reduced relative to WT RTA in cells transfected with RTA mutant constructs

To determine if endogenously expressed RTA and RTA mutants depurinate rRNA in transfected MAC-T cells, total RNA was collected 19 h after transfection and a dual primer extension assay was performed (Fig. 3A). Since the dual primer extension assay is relatively semi-quantitative we also established a qRT-PCR assay to determine ribosome depurination (Fig. 3B). As shown in Table S1, the results obtained with dual primer extension were matched closely by qRT-PCR . In general, the levels of depurination in cells transfected with preRTA constructs were similar to those in cells transfected with the mature RTA counterpart. All mutants tested depurinated MAC-T rRNA significantly less than their WT control with the exception of mature P95L. The reduction in depurination was the most marked with the active site mutants E177Q and E177K which depurinated less than 40% and 20%, respectively, relative to their WT controls. Ribosome depurination was 60 to 70% of that observed for WT RTA for E145K, P95L/E145K, S215F and G212E.

A GFP transfection assay was used to determine if protein synthesis inhibition corresponded with changes in ribosome depurination. Overall, the pattern of ribosome depurination observed with the mutated RTA proteins was reflected in the degree of protein synthesis inhibition (Fig. 4). Fluorescence was almost nondetectable in cells transfected with pre- or mature WT RTA relative to cells transfected with plasmid vector alone. Similar results were obtained with P95L, which depurinated ribosomes similarly to WT RTA based on qRT-PCR results. Pre- and mature E177K did not inhibit protein synthesis which corresponded with the very slight degree of depurination observed. Protein synthesis levels observed with pre- and mature E177Q were intermediate between E177K and the other mutants. Surprisingly, a greater level of inhibition of protein synthesis was observed with mature E177Q (60% inhibition of vector controls) compared to preE177Q (40% inhibition of vector controls) even though they showed similar levels of depurination at 19 h after transfection. Protein synthesis was inhibited significantly less relative to WT RTA for preP95L/E145K and for pre- and mature S215F and G212E, however, this still represented an 80 to 90% inhibition of protein synthesis relative to vector controls. Interestingly, the mature RTA mutants tended to have a greater effect on protein synthesis inhibition than their preRTA counterparts. Specifically, preE177Q, P95L/E145K, S215F and G212E inhibited protein synthesis less than their corresponding mature forms and less than WT preRTA.

3.3. Activation of apoptosis corresponds with protein synthesis inhibition in cells transfected with RTA and RTA mutant constructs

To investigate if apoptosis was induced in the transfected cells, activation of caspase 3/7 was investigated in MAC-T cells 19 h after transfection (Fig. 5). Caspase activity was induced similarly by pre- and mature WT RTA (2.7 ± 0.2 and 2.8 ± 0.2-fold, respectively; mean ± SE of 9 experiments) relative to vector controls. The active site mutant E177K elicited negligible caspase activation which corresponded with the lack of ribosome depurination and protein synthesis inhibition. In contrast the pre- and mature forms of E145K, G212E and P95L/E145K as well as mature S215F activated caspase activity to the same degree as their respective WT RTA controls. PreS215F activated caspase 3/7 to a lesser extent than WT preRTA, which corresponded with decreases in depurination and protein synthesis inhibition. The E177Q mutant also showed a difference between the pre- and mature forms in terms of caspase activation, with mature E177Q eliciting a greater increase in caspase 3/7 activity relative to preE177Q. Interestingly, both the pre- and mature forms of P95L activated caspase to a greater extent relative to their WT counterparts.

As a second indicator of apoptosis, a nucleosome accumulation assay was conducted (Fig. 6). Wild-type pre- and mature RTA each increased nucleosome accumulation two-fold over cells transfected with vector alone. While there was more variability with this assay, the results mirrored overall those of the caspase assay. Mature E177Q had more activity than pre E177Q while neither form of E177K showed any activity. The other mutants also showed activity that was similar to what was observed with the caspase assay.

RTA has been shown to activate JNK and p38 signaling pathways in MAC-T cells (Jetzt et al., 2009), therefore the ability of the different mutants to activate these pathways was examined (Fig. 7). Endogenous expression of both pre- and mature RTA activated JNK and p38 approximately 2-fold relative to vector alone. However, neither JNK nor p38 was activated by expression of pre- or mature E177K. Mutants E145K, G212E, P95L/E145K and S215F activated JNK and p38 signaling similarly to WT RTA controls. This corresponded with full caspase activation with the exception of preS215F, which exhibited decreases in caspase activation. Interestingly, the ability of the active site mutant E177Q to activate JNK and p38 appeared intermediate between E177K and the other mutants.

4. Discussion

4.1. Development of a mammalian expression system to study biological activity of pre- and mature WT RTA and RTA mutants

This is the first report where catalytically active WT RTA and RTA mutants have been expressed in mammalian cells to study the relationship between depurination, protein synthesis inhibition, cell signaling and apoptosis. By optimizing codon usage for the bovine, we were able to increase expression such that we could detect RTA protein by immunoblot analysis in 25 to 50 μg total cell lysates from either bovine or human cells using a specific RTA antibody. Redmann and coworkers (Redmann et al., 2011) recently reported the expression of preRTA and two preRTA mutants in mammalian cells. In their study an N-terminal murine MHC class I heavy chain H2-K^b signal peptide was used to target an enzymatically attenuated RTA variant to the ER membrane. Also, RTA trafficking was the main endpoint studied in that report and the enzymatically attenuated RTA variant was expressed with an HA epitope tag for detection by immunoprecipitation. Using the native signal peptide of ricin, we successfully targeted RTA to the ER membrane in mammalian cells as shown by production of glycosylated protein. The mature form of RTA was not glycosylated, indicating that it was not translocated into the ER. The mature form served as a control to detect changes in catalytic activity, since changes in depurination by mature RTA would be due to catalytic activity and not to trafficking. At the time point measured,

levels of depurination were similar between pre- and mature forms of RTA, indicating that preRTA successfully trafficked from the ER to the ribosome.

E177 has been identified as an invariant amino acid across the RIP family. It lies within the active site of RTA and is known to be a key catalytic residue (Monzingo and Robertus, 1992). In the present study, conversion of E177 to lysine (E177K) produced mutants that exhibited virtually no detectable depurination activity and failed to inhibit protein synthesis, induce apoptosis or activate signaling of the JNK and p38 cascades. This agrees with results obtained with other systems, e.g., this mutation led to total inactivation of the enzyme in an *in vitro* translation assay (Chaddock and Roberts, 1993) and allowed growth in yeast (Allen et al., 2005, Li et al., 2007). Pre- and mature E177K were expressed at the highest level relative to all other constructs. Interestingly, in a study where amino acids were systematically deleted to determine their role in RTA activity, an inverse correlation was observed between expression in *E. coli* and enzymatic activity *in vitro* (Morris and Wool, 1992). This suggests that the very high level of E177K expression may be related to complete lack of biological activity of the mutant protein. These results are also consistent with previous studies in yeast (Li et al., 2007) and suggest that greater enzymatic activity of RTA will lead to higher translation inhibition and reduced protein accumulation.

4.2. A substantial reduction in depurination is necessary to prevent inhibition of translation by RTA in mammalian cells

In yeast, we found that S215F and P95L/E145K induced depurination and inhibited protein synthesis similarly to WT preRTA but did not induce nuclear fragmentation and ROS generation, hallmarks of apoptosis. In addition, G212E had low biological activity and did not affect any of these endpoints (Li et al., 2007). Expression of pre- and mature forms of each of these three mutants reduced depurination levels to 60% of WT RTA control levels in mammalian cells at 19 h after transfection. This lower level of depurination was still sufficient to inhibit protein synthesis by 80 to 90% relative to the vector control. Interestingly, the pre-forms of G212E, S215F, and P95L/E145K did tend to have higher levels of protein synthesis compared to the mature forms or WT preRTA when expressed in mammalian cells, although protein synthesis was still only 15 to 20% of vector control levels. However, they produced full caspase activation, nucleosome accumulation and JNK/p38 signaling. These results indicate that depurination can be reduced by as much as 40% in mammalian cells with minimal effects on protein synthesis inhibition and activation of stress-activated signaling cascades and apoptosis. A substantial reduction in depurination as was observed with pre E177Q may be necessary to prevent protein synthesis inhibition by RTA, possibly due to the high sensitivity of mammalian ribosomes to RTA.

4.3. Activation of apoptosis by RTA mutants corresponds better with the extent of protein synthesis inhibition than depurination in mammalian cells

Since E177K exhibited virtually no biological activity, we converted Glu177 to glutamine (E177Q) with the goal of producing an active site mutant that retained some biological activity. This resulted in the expression of pre- and mature RTA proteins that exhibited depurination activity that was approximately 35% of that observed with WT RTA. This agrees with previous studies (Ready et al., 1991) demonstrating that the E177Q mutation decreases enzymatic activity at least 170-fold relative to WT RTA *in vitro* but less than that of the E177K mutation. Interestingly, while ribosome depurination was similar between the pre- and mature forms of E177Q, the degree of protein synthesis inhibition as well as the induction of apoptosis differed. For the pre form of E177Q, protein synthesis was reduced 32% relative to vector control. However, apoptosis was not induced. In contrast, the mature form of E177Q inhibited protein synthesis 60% relative to vector contols which corresponded with full caspase activation and nucleosome accumulation. The reason for the

difference in the degree of protein synthesis inhibition when depurination levels were similar is unknown at this time, but may be related to differences in the rate of depurination (Yan et al., 2012). These results indicate that there may be a threshold level of protein synthesis inhibition that correlates with activation of apoptosis in mammalian cells. Interestingly, the difference in the activation of apoptosis did not appear to correlate with differences in activation of JNK or p38, since JNK activation was statistically less for mature E177Q compared to the pre form and there was no difference between the two for p38 activation. Recently it was reported that ricin mediates IL-1β release from bone-marrow derived macrophages through a scaffolding complex termed the NALP3 inflammasome, which facilitates cleavage of pro-IL-1β to active IL-1β by caspase-1. Using inhibitors for proteosome degradation and the JNK and p38 pathways it was concluded that ricin-mediated translation inhibition caused the disappearance of labile proteins that normally suppress inflammasome formation independent of JNK and p38 kinase activation (Lindauer et al., 2010). Therefore protein synthesis inhibition itself may mediate RTA-induced apoptosis through mechanisms that are independent of stress kinases.

In summary, we have successfully expressed pre- and mature forms of RTA in mammalian cells that retain biological activity. This was achieved by optimizing the codon usage of RTA for bovine ribosomes. We present evidence that a relatively low level of depurination by RTA can trigger protein synthesis inhibition, apoptosis and stress-activated signaling, indicating that a substantial reduction in depurination is necessary to prevent protein synthesis inhibition by RTA in mammalian cells. Our results show that protein synthesis inhibition correlates more linearly with apoptosis than the level of depurination. Further studies are warranted to identify the specific link between protein synthesis inhibition and apoptosis in RTA-treated cells.

Supplementary Material

Refer to Web version on PubMed Central for supplementary material.

Acknowledgments

The authors thank Dr. M. Porotto, Weill Cornell Medical College, New York, NY for supplying the pCAGGS mammalian expression vector and Kerrie May and Jennifer Nielsen-Kahn for helpful comments. We thank NIAID NIH Biodefense and Emerging Infections (BEI) Research Resources Repository (Manassas, VA) for recombinant RTA with N-terminal histidine tag expressed in *E. coli* (NR-853). This work was supported by National Institutes of Health grant AI059720 to N.E.T. and W.S.C.

Abbreviations

FBS	fetal bovine serum
JNK	c-Jun N-terminal kinase
PVDF	polyvinylidene fluoride
RIP	ribosome-inactivating protein
RTA	ricin toxin A chain
RTB	ricin toxin B chain

References

Allen SC, Byron A, Lord JM, Davey J, Roberts LM, Ladds G. Utilisation of the budding yeast Saccharomyces cerevisiae for the generation and isolation of non-lethal ricin A chain variants. Yeast. 2005; 22:1287–97. [PubMed: 16358307]

Audi J, Belson M, Patel M, Schier J, Osterloh J. Ricin poisoning: a comprehensive review. JAMA. 2005; 294:2342–51. [PubMed: 16278363]

Castelletti D, Fracasso G, Righetti S, Tridente G, Schnell R, Engert A, et al. A dominant linear B-cell epitope of ricin A-chain is the target of a neutralizing antibody response in Hodgkin's lymphoma patients treated with an anti-CD25 immunotoxin. Clin Exp Immunol. 2004; 136:365–72. [PubMed: 15086403]

Chaddock JA, Roberts LM. Mutagenesis and kinetic analysis of the active site Glu177 of ricin A-chain. Protein Eng. 1993; 6:425–31. [PubMed: 8332600]

Dai J, Zhao L, Yang H, Guo H, Fan K, Wang H, et al. Identification of a novel functional domain of ricin responsible for its potent toxicity. J Biol Chem. 2011; 286:12166–71. [PubMed: 21303906]

Fleming J, Leibowitz BJ, Kerr DE, Cohick WS. IGF-I differentially regulates IGF binding protein expression in primary mammary fibroblasts and epithelial cells. J Endocrinol. 2005; 186:165–78. [PubMed: 16002546]

Grill CJ, Sivaprasad U, Cohick WS. Constitutive expression of IGF-binding protein-3 by mammary epithelial cells alters signaling through Akt and p70S6 kinase. J Mol Endocrinol. 2002; 29:153–62. [PubMed: 12200236]

Halling KC, Halling AC, Murray EE, Ladin BF, Houston LL, Weaver RF. Genomic cloning and characterization of a ricin gene from Ricinus communis. Nucleic Acids Res. 1985; 13:8019–33. [PubMed: 2999712]

Higuchi S, Tamura T, Oda T. Cross-talk between the pathways leading to the induction of apoptosis and the secretion of tumor necrosis factor-alpha in ricin-treated RAW 264. 7 cells. J Biochem. 2003; 134:927–33. [PubMed: 14769883]

Hu R, Zhai Q, Liu W, Liu X. An insight into the mechanism of cytotoxicity of ricin to hepatoma cell: roles of Bcl-2 family proteins, caspases, Ca(2+)-dependent proteases and protein kinase C. J Cell Biochem. 2001; 81:583–93. [PubMed: 11329613]

Huynh HT, Robitaille G, Turner JD. Establishment of bovine mammary epithelial cells (MAC-T): an in vitro model for bovine lactation. Exp Cell Res. 1991; 197:191–99. [PubMed: 1659986]

Iordanov MS, Pribnow D, Magun JL, Dinh TH, Pearson JA, Chen SL, et al. Ribotoxic stress response: activation of the stress-activated protein kinase JNK1 by inhibitors of the peptidyl transferase reaction and by sequence-specific RNA damage to the alpha-sarcin/ricin loop in the 28S rRNA. Mol Cell Biol. 1997; 17:3373–81. [PubMed: 9154836]

Jetzt AE, Cheng JS, Tumer NE, Cohick WS. Ricin A-chain requires c-Jun N-terminal kinase to induce apoptosis in nontransformed epithelial cells. Int J Biochem Cell Biol. 2009; 41:2503–10. [PubMed: 19695342]

Jolliffe NA, Di Cola A, Marsden CJ, Lord JM, Ceriotti A, Frigerio L, et al. The N-terminal ricin propeptide influences the fate of ricin A-chain in tobacco protoplasts. J Biol Chem. 2006; 281:23377–85. [PubMed: 16774920]

Kageyama A, Kusano I, Tamura T, Oda T, Muramatsu T. Comparison of the apoptosis-inducing abilities of various protein synthesis inhibitors in U937 cells. Biosci Biotechnol Biochem. 2002; 66:835–9. [PubMed: 12036057]

Korcheva V, Wong J, Lindauer M, Jacoby DB, Iordanov MS, Magun B. Role of apoptotic signaling pathways in regulation of inflammatory responses to ricin in primary murine macrophages. Mol Immunol. 2007; 44:2761–71. [PubMed: 17257680]

Li XP, Baricevic M, Saidasan H, Tumer NE. Ribosome depurination is not sufficient for ricin-mediated cell death in Saccharomyces cerevisiae. Infect Immun. 2007; 75:417–28. [PubMed: 17101666]

Lindauer M, Wong J, Magun B. Ricin toxin activates the NALP3 inflammasome. Toxins (Basel). 2010; 2:1500–14. [PubMed: 20862209]

Marsden CJ, Knight S, Smith DC, Day PJ, Roberts LM, Phillips GJ, et al. Insertional mutagenesis of ricin A chain: a novel route to an anti-ricin vaccine. Vaccine. 2004; 22:2800–5. [PubMed: 15246614]

Melchior WB Jr, Tolleson WH. A functional quantitative polymerase chain reaction assay for ricin, Shiga toxin, and related ribosome-inactivating proteins. Anal Biochem. 2010; 396:204–11. [PubMed: 19766090]

Monzingo AF, Robertus JD. X-ray analysis of substrate analogs in the ricin A-chain active site. J Mol Biol. 1992; 227:1136–45. [PubMed: 1433290]

Morris KN, Wool IG. Determination by systematic deletion of the amino acids essential for catalysis by ricin A chain. Proc Natl Acad Sci U S A. 1992; 89:4869–73. [PubMed: 1594586]

Niwa H, Yamamura K, Miyazaki J. Efficient selection for high-expression transfectants with a novel eukaryotic vector. Gene. 1991; 108:193–9. [PubMed: 1660837]

Pang YP, Park JG, Wang S, Vummenthala A, Mishra RK, McLaughlin JE, et al. Small-molecule inhibitor leads of ribosome-inactivating proteins developed using the doorstop approach. PLoS One. 2011; 6:e17883. [PubMed: 21455295]

Piatak M, Lane JA, Laird W, Bjorn MJ, Wang A, Williams M. Expression of soluble and fully functional ricin A chain in Escherichia coli is temperature-sensitive. J Biol Chem. 1988; 263:4837–43. [PubMed: 3280569]

Pruet JM, Jasheway KR, Manzano LA, Bai Y, Anslyn EV, Robertus JD. 7-Substituted pterins provide a new direction for ricin A chain inhibitors. Eur J Med Chem. 2011

Rainey GJ, Young JA. Antitoxins: novel strategies to target agents of bioterrorism. Nat Rev Microbiol. 2004; 2:721–6. [PubMed: 15372082]

Rao PV, Jayaraj R, Bhaskar AS, Kumar O, Bhattacharya R, Saxena P, et al. Mechanism of ricin-induced apoptosis in human cervical cancer cells. Biochem Pharmacol. 2005; 69:855–65. [PubMed: 15710362]

Rapak A, Falnes PO, Olsnes S. Retrograde transport of mutant ricin to the endoplasmic reticulum with subsequent translocation to cytosol. Proc Natl Acad Sci U S A. 1997; 94:3783–8. [PubMed: 9108055]

Ready MP, Kim Y, Robertus JD. Site-directed mutagenesis of ricin A-chain and implications for the mechanism of action. Proteins. 1991; 10:270–8. [PubMed: 1881883]

Redmann V, Oresic K, Tortorella LL, Cook JP, Lord M, Tortorella D. Dislocation of ricin toxin A chains in human cells utilizes selective cellular factors. J Biol Chem. 2011; 286:21231–8. [PubMed: 21527639]

Rutenber E, Katzin BJ, Ernst S, Collins EJ, Mlsna D, Ready MP, et al. Crystallographic refinement of ricin to 2.5 A. Proteins. 1991; 10:240–50. [PubMed: 1881880]

Sandvig K, van Deurs B. Delivery into cells: lessons learned from plant and bacterial toxins. Gene Ther. 2005; 12:865–72. [PubMed: 15815697]

Schindler J, Gajavelli S, Ravandi F, Shen Y, Parekh S, Braunchweig I, et al. A phase I study of a combination of anti-CD19 and anti-CD22 immunotoxins (Combotox) in adult patients with refractory B-lineage acute lymphoblastic leukaemia. Br J Haematol. 2011; 154:471–6. [PubMed: 21732928]

Smallshaw JE, Richardson JA, Vitetta ES. RiVax, a recombinant ricin subunit vaccine, protects mice against ricin delivered by gavage or aerosol. Vaccine. 2007; 25:7459–69. [PubMed: 17875350]

Smallshaw JE, Vitetta ES. Ricin vaccine development. Curr Top Microbiol Immunol. 2012; 357:259–72. [PubMed: 21805396]

Spooner RA, Lord JM. How ricin and Shiga toxin reach the cytosol of target cells: retrotranslocation from the endoplasmic reticulum. Curr Top Microbiol Immunol. 2012; 357:19–40. [PubMed: 21761287]

Stechmann B, Bai SK, Gobbo E, Lopez R, Merer G, Pinchard S, et al. Inhibition of retrograde transport protects mice from lethal ricin challenge. Cell. 2010; 141:231–42. [PubMed: 20403321]

Tesh VL. The induction of apoptosis by Shiga toxins and ricin. Curr Top Microbiol Immunol. 2012; 357:137–78. [PubMed: 22130961]

Vitetta ES, Smallshaw JE, Coleman E, Jafri H, Foster C, Munford R, et al. A pilot clinical trial of a recombinant ricin vaccine in normal humans. Proc Natl Acad Sci U S A. 2006; 103:2268–73. [PubMed: 16461456]

Wahome PG, Bai Y, Neal LM, Robertus JD, Mantis NJ. Identification of small-molecule inhibitors of ricin and shiga toxin using a cell-based high-throughput screen. Toxicon. 2010; 56:313–23. [PubMed: 20350563]

Watson P, Spooner RA. Toxin entry and trafficking in mammalian cells. Adv Drug Deliv Rev. 2006; 58:1581–96. [PubMed: 17118486]

Yan Q, Li X-P, Tumer NE. N-glycosylation does not affect the catalytic activity of ricin A chain but stimulates cytotoxicity by promoting its transport out of the endoplasmic reticulum. Traffic. 2012 [Epub ahead of print]. 10.1111/j.1600-0854.2012.01404.x

Zhou XX, Ji F, Zhao JL, Cheng LF, Xu CF. Anti-cancer activity of anti-p185HER-2 ricin A chain immunotoxin on gastric cancer cells. J Gastroenterol Hepatol. 2010; 25:1266–75. [PubMed: 20594254]

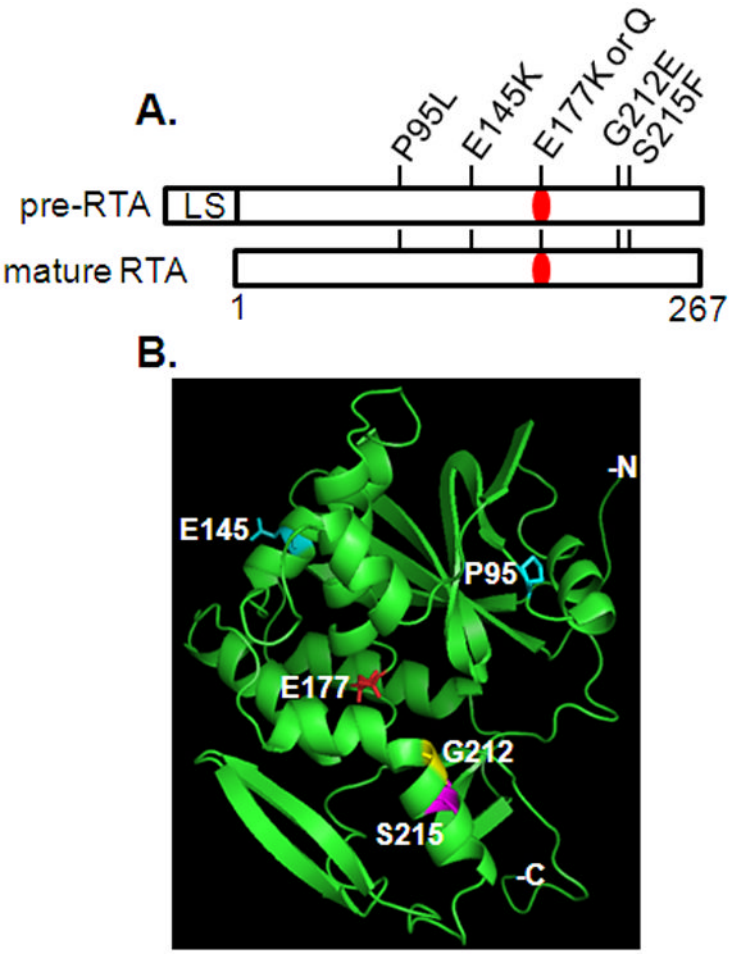

Figure 1.

Protein structure of RTA showing mutations analyzed in the current study. **A.** Linear schematic representation of RTA. Numbers refer to amino acid residue in mature RTA. LS represents the 35-residue leader peptide containing the 26-residue signal sequence and a 9-residue propeptide (Jolliffe et al., 2006). The SS is present in preRTA but not mature RTA. The active site is shown in red. **B.** Three-dimensional structure of mature RTA. Active site residue E177 is shown in red, P95 and E145are shown in cyan, G212 is shown in yellow, and S215is shown in magenta. RTA structure is form Protein Data Bank ID 1RTC. The amino (N) and carboxy (C) termini and the mutations were labeled using the PyMOL Molecular Graphics System, Schrödinger, LLC.

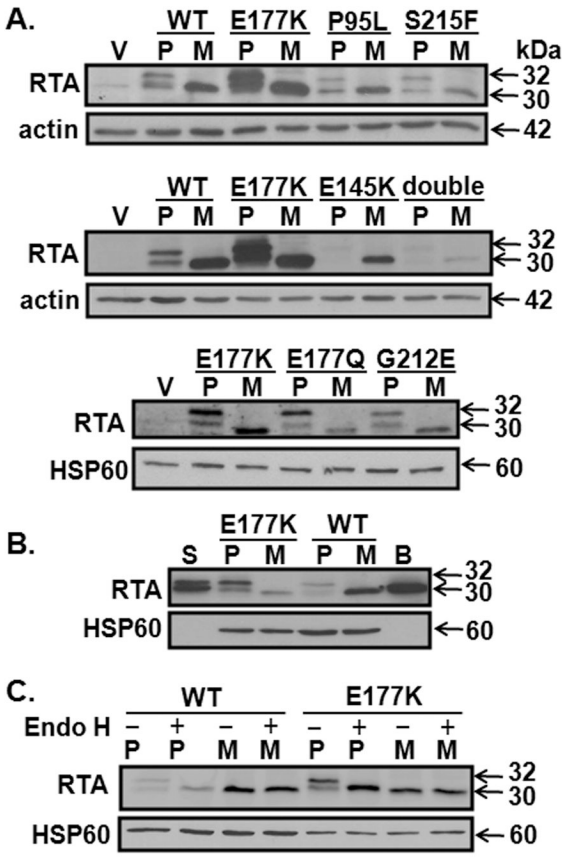

Figure 2.

Expression of RTA and RTA mutants in transfected MAC-T cells. Total cell lysates (**A.** 50 μg per lane; **B.** 50 μg per lane for vector and wt; 25 μg for E177K) were collected from MAC-T cells 19 h after transfection. Membranes were immunoblotted with anti-RTA antibody then stripped and reprobed with antibodies to actin or HSP60. Blots are representative of 2 to 3 experiments. S = RTA glycosylated standard from Sigma (5 ng); B = non-glycosylated RTA standard from BEI (10 ng). **C.** Total cell lysates (40 μg for WT and 20 μg for E177K) were treated with Endo H prior to immunoblotting. V = vector; P = pre; M = mature; WT = wild-type; double = P95L/E145K.

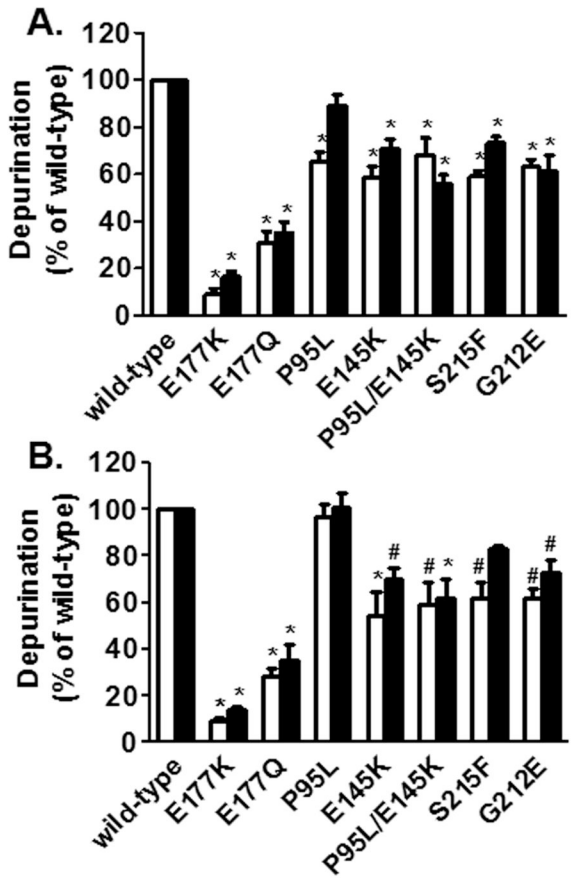

Figure 3.

Ribosome depurination by endogenously expressed RTA and RTA mutants in MAC-T cells. **A.** Total RNA was collected 19 h after transfection and analyzed by dual primer extension. Dual primer extension products were separated on a 7 M urea−5% polyacrylamide denaturing gel. Bands were visualized and quantified by PhosphorImager (GE Healthcare). Depurination was normalized against total 28S rRNA. **B.** Total RNA was collected 19 h after transfection and analyzed by qRT-PCR. Bars represent mean ± S.E. of at least three experiments. White bars = preRTA constructs; black bars = mature RTA constructs. Significance compared to pre or mature WT RTA is indicated as: *, $P < 0.001$; #, $P < 0.01$.

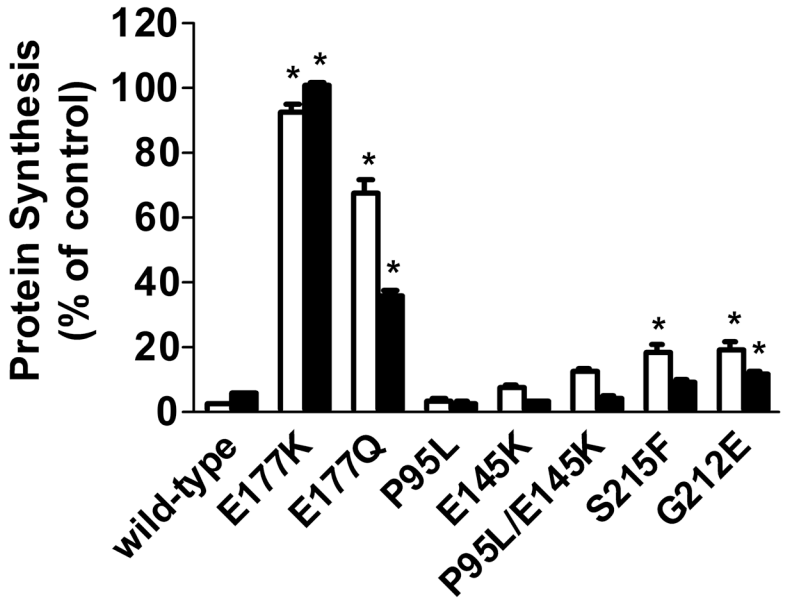

Figure 4.

Protein synthesis in cells transfected with endogenously expressed RTA and RTA mutants in MAC-T cells. Fluorescence was measured 21 h after co-transfection of RTA or RTA mutants and pEGFP. Fluorescence measured in cells co-transfected with pEGFP and empty vector was considered 100%. Each bar represents mean ± S.E. of three experiments, with each treatment performed in triplicate within an experiment. White bars = preRTA constructs; black bars = mature RTA constructs. Significance compared to pre or mature WT RTA is indicated as: *, $P < 0.001$; ‡, $P < 0.05$.

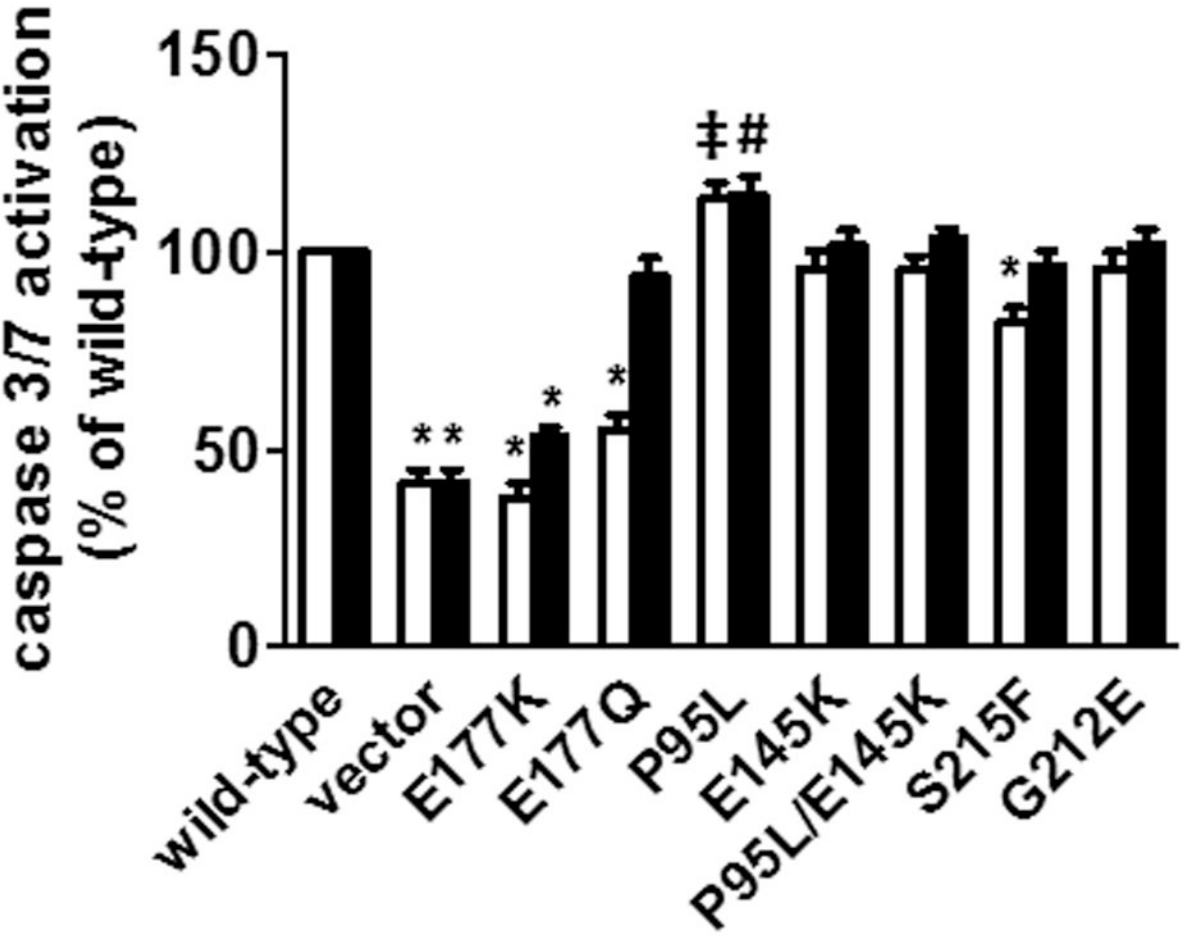

Figure 5.

Caspase 3/7 activation by endogenously expressed RTA and RTA mutants in MAC-T cells. Caspase 3/7 activity was measured 19 h after transfection using the fluorescent SensoLyte Homogeneous AMC Caspase 3/7 Assay kit (AnaSpec). Bars represent mean ± S.E. of at least six experiments. White bars = preRTA constructs; black bars = mature RTA constructs. Significance compared to pre or mature WT RTA is indicated as: *, $P < 0.001$; #, $P < 0.01$; ‡, $P < 0.05$.

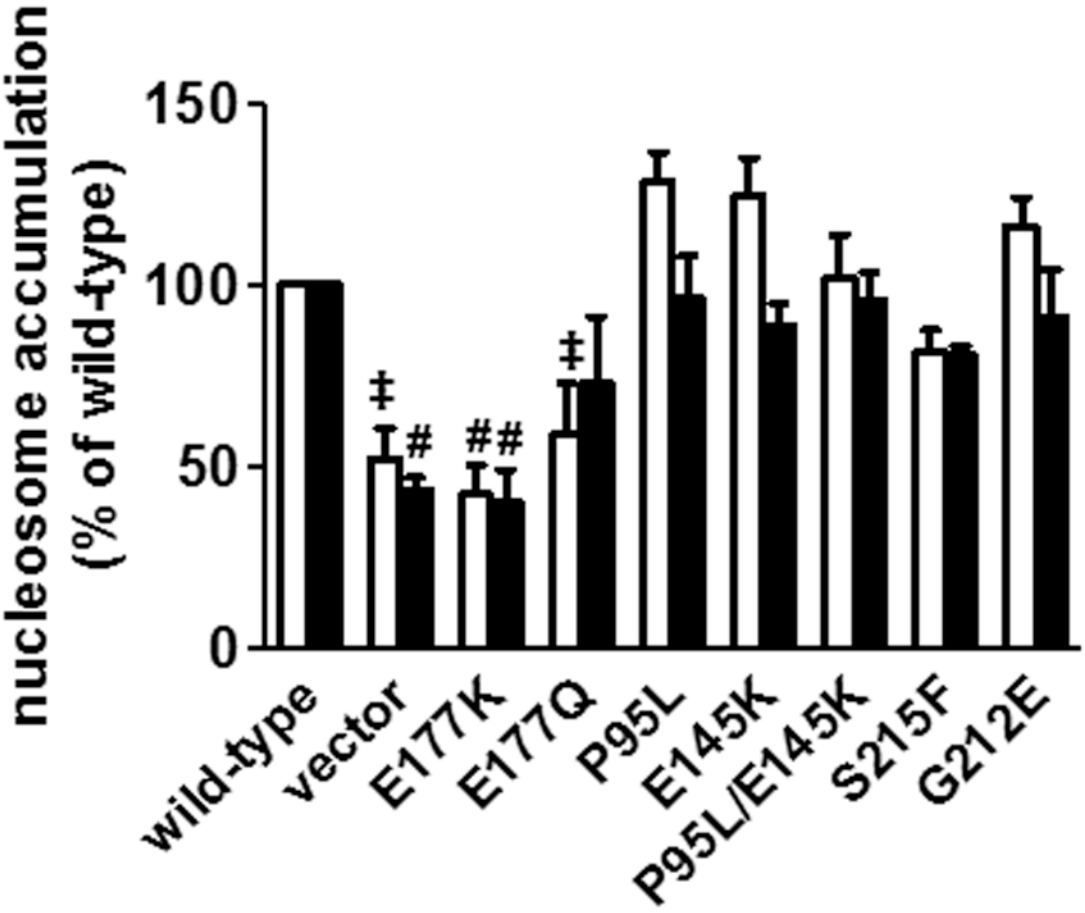

Figure 6.

Nucleosome accumulation by endogenously expressed RTA and RTA mutants in MAC-T cells. Nucleosome accumulation was measured 19 h after transfection using the Cell Death Detection ELISA^{PLUS} kit (Roche). Bars represent mean ± S.E. of three experiments. White bars = preRTA constructs; black bars = mature RTA constructs. Significance compared to pre or mature WT RTA is indicated as: #, $P < 0.01$; ‡, $P < 0.05$.

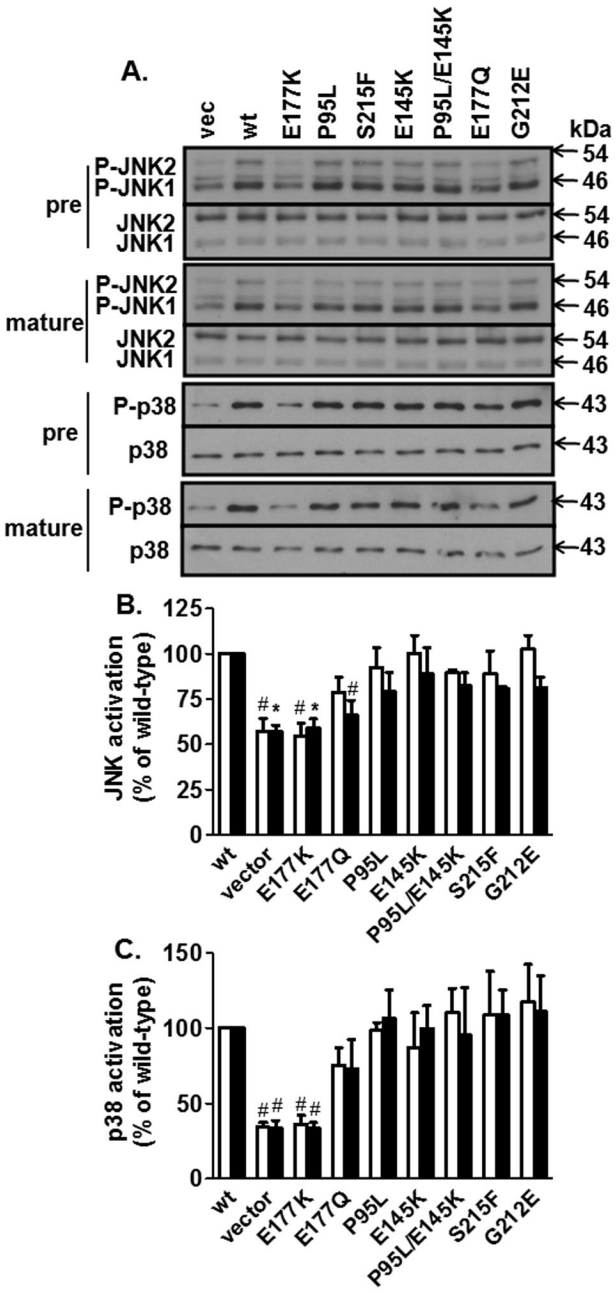

Figure 7.

Activation of JNK and p38 by endogenously expressed RTA and RTA mutants in MAC-T cells. **A.** Total cell lysates (30 μg) were collected 19 h after transfection, separated by SDS-PAGE, and immunoblotted with P-JNK or P-p38 antibodies. Membranes were stripped and reprobed with antibodies to JNK or p38. **B.** and **C.** Bands were quantitated by densitometry. Bars represent mean ± S.E. of at least three experiments. White bars = preRTA constructs; black bars = mature RTA constructs. Vec = vector; WT = wild-type. Significance compared to pre or mature WT RTA is indicated as *, $P < 0.001$; #, $P < 0.01$.